



Contents lists available at ScienceDirect

Spectrochimica Acta Part A: Molecular and Biomolecular Spectroscopy

journal homepage: www.elsevier.com/locate/saa

Development of the fluorescent carbon nanosensor for pH and temperature of liquid media with artificial neural networks



O.E. Sarmanova^{a,*}, K.A. Laptinskiy^{a,b}, M.Yu. Khmeleva^{a,b}, S.A. Burikov^{a,b}, S.A. Dolenko^b, A.E. Tomskaya^c, T.A. Dolenko^{a,b}

^a Department of Physics, Lomonosov Moscow State University, Moscow 119991, Russia

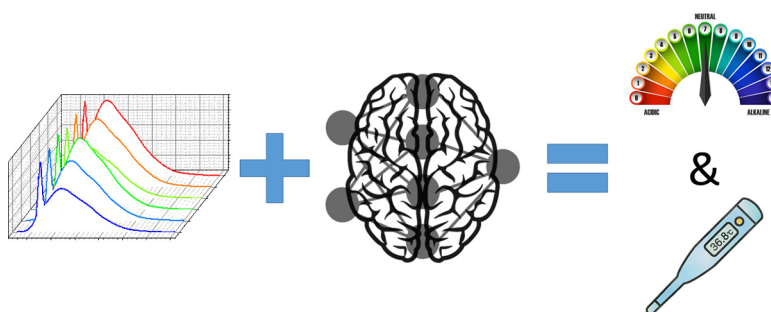
^b Skobeltsyn Institute of Nuclear Physics, Lomonosov Moscow State University, Moscow 119991, Russia

^c North-Eastern Federal University, Yakutsk 677007, Russia

HIGHLIGHTS

- Fluorescent nanosensor is developed for simultaneous pH and temperature measurement.
- The nanosensors are carbon dots (CD) synthesized via hydrothermal method.
- Neural networks provide pH and temperature measurement with 0.005 and 0.67 °C error.
- Developed CD-based nanosensor operates in temperature range 22–81 °C of environment.
- Developed nanosensor provides pH measurement exceeding nanoscale analogs accuracy.

GRAPHICAL ABSTRACT



ARTICLE INFO

Article history:

Received 18 December 2020
 Received in revised form 14 April 2021
 Accepted 16 April 2021
 Available online 21 April 2021

Keywords:

Carbon dots
 Fluorescence spectroscopy
 Artificial neural networks
 nanosensor for pH and temperature

ABSTRACT

The present study is devoted to the creation of optical nanosensors for pH and temperature of liquid media based on carbon dots (CD) prepared via hydrothermal synthesis. The application of artificial neural networks to the CD fluorescence spectra database provided simultaneous determination of pH and ambient temperature values with an accuracy of 0.005 pH units and 0.67 °C, respectively. The obtained results are unique since they indicate the possibility of creating a multifunctional CD-based nanosensor that operates in a wide temperature range (22–81 °C) and provides an accuracy of pH determination exceeding the accuracy of nanoscale analogs by an order of magnitude.

© 2021 Elsevier B.V. All rights reserved.

1. Introduction

Due to the rapid technological progress and continuous improvement of knowledge in the field of natural sciences, the most promising approaches are those involving the diagnosis and treatment of diseases at the molecular level. To implement these

approaches, one requires special instrumentation to monitor the state of the body at the cellular level. For example, in many cellular processes, such as proliferation, apoptosis, ion transport, calcium regulation, etc. [1], pH plays a crucial role. A shift in the human blood pH by 0.1 units beyond the reference values (7.35–7.45) causes severe respiratory, cardiovascular disorders, etc., and a shift by 0.4 units often leads to a lethal outcome [2]. For a typical mammalian cell, the intracellular pH value ranges from 4.7 to 8.0, and its change can lead to a functional disorder of the organelles [3].

* Corresponding author.

E-mail address: oe.sarmanova@physics.msu.ru (O.E. Sarmanova).

Usually, an abnormal intracellular pH value is a characteristic of many common diseases, such as Alzheimer's disease, apoplexy, and cancer [4]. To date, several methods have been proposed for monitoring the pH value at the cellular level. In [5], one used a fluorescent probe based on naphthalimide-rhodamine to determine the pH value in cells. Its operational principle is based on fluorescence (FL) resonance energy transfer between various fluorophores of the complex depending on pH. This sensor determines the pH value in the range from 4.02 to 4.63 with an accuracy of 0.05 pH units. In the study [6], a complex of 2-(6-(4-aminostyryl)-1,3-dioxo-1H-benzo[de]isoquinoline-2(3H)-yl)-N, N-dimethylethanamine was synthesized. It allows determining the pH value of the intracellular environment by detecting the FL alterations of the complex. The pH measurement span of the nanoprobe encompasses the range from 3 to 6 units.

Another crucial factor characterizing the state of the cell is temperature [7]. Monitoring the temperature at the cellular level is essential for photothermal therapy [8]. Moreover, temperature changes may indicate the presence of inflammatory processes in the body [7]. To date, various methods for determining temperature at the cellular level have been proposed. For example, in [9] one suggested using rare-earth-based nanoparticles to determine the temperature in the biological media. The accuracy of temperature determination in [9] was 0.73°C in the temperature range of 24–44 °C. The paper [10] proposed to use green fluorescent proteins to monitor the temperature in the cell volume. The authors demonstrated high accuracy of temperature determination – 0.4°C in the temperature range of 20–60°C.

Despite the active development of the cellular nanosensors, the task of creating a sensor that can simultaneously determine several parameters of the cellular environment remains challenging. Carbon dots (CD) synthesized over the past decade meet many requirements for biomedical agents, such as non-toxicity, biocompatibility [11], sensitivity of their FL to changes in the environment (in the presence of various ions [12], due to the temperature [13] or pH changes [14], in various solvents [15]), and have good prospects for application in biomedicine. There are known studies investigating the possibility of using CD as a cellular nanosensor of temperature [13] and pH [14]. Thus, CD prepared via microwave synthesis in [13] showed a linear dependence of their FL intensity on the temperature in the range of 5–60 °C. Under heating HeLa cells with incubated CD, an increase in the brightness of the image in the microscope was observed. In the paper [14], one demonstrated the application of CD synthesized via hydrothermal method as a pH sensor. The FL intensity of the obtained CD linearly decreased with increasing pH from 4 to 8 units. The analysis of fluorescent microscope images of HeLa cells incubated with CD, allowed to establish the difference of pH values between cytosol and lysosomes. However, the authors of the present article could not find publications concerning the creation of CD-based cellular fluorescent nanosensors that can simultaneously determine several environmental parameters. The way to solve this multiparametric inverse problem of fluorescence spectroscopy is to use artificial neural networks (ANN).

The recent decade witnessed ANN becoming actively implemented to solve problems of medical diagnostics, including those implying the solution of optical spectroscopy inverse problems. Thus, in papers [16], Raman spectra of biological tissues were processed via ANNs in order to improve the accuracy of brain cancer diagnosis. Structural changes in proteins and lipids in cancer tissue resulted in alterations of Raman spectra, which allowed to distinguish healthy cells from affected ones. There are numerous works where ANNs are used to solve multiparametric inverse problems of monitoring a biosystem state. In the paper [17], the content of nutrients, metabolites, and viable cell concentration in culture

media of BHK-21 cell line was simultaneously determined using perceptrons from the UV–VIS absorption spectra of phenol red.

The authors of the present study have numerously demonstrated the success of the neural network approach in solving inverse problems of optical spectroscopy – problems for determining the presence and concentration of carbon nanoagents based on Raman spectra, fluorescence, and absorption of biological media with nanoagents injected into them [18,19].

There are few studies applying ANNs to create fluorescent nanosensors. In the article [20], the authors evaluated the performance of CdSe/ZnS quantum dots as fluorescent thermometers deposited on the surface of optical fiber. The inverse problem of temperature determination from the FL spectra of quantum dots was solved using experiment-based and quasi-model approaches. In the first case, one used experimental data to train ANN – peak and integral FL intensity values, the wavelength of FL maximum, FWHM value, etc. In the second case, simulated spectra were used in order to obtain representative data sets. The root mean squared error (RMSE) for temperature detection was 1.1 K for the first approach and 0.29 K for the quasi-model approach. In paper [21], one developed an optical pH sensor based on N-doped CD, operating in pH values range from 2.0 to 14.0. Application of back-propagation ANN allowed determining the pH of nanoparticles aqueous suspension with an RMSE of cross-validation of 0.067 units, which was 0.85% of the average pH value.

This paper considers the possibility of simultaneous determination of the liquid medium pH and temperature values via CD FL spectra. High sensitivity of CD fluorescence prepared via hydrothermal synthesis towards changes in the specified environment parameters was found. In this study back-propagation ANNs were used to solve the two-parameter inverse problem of pH and temperature determination on the spectra of CD FL.

2. Materials and methods

2.1. Objects of research

In this study CD particles obtained via the method described in [22] were used. Citric acid powder was dissolved in the aqueous solution of ammonia (30%) and in 20 ml of deionized water. The solution was processed in the ultrasonic bath for 5–10 min and then the mixture was kept for 2 h at the temperature 190 °C in autoclave. In order to isolate CD nanoparticles and remove synthesis byproducts, the suspension was filtered through the track membrane with the pore size of 100 nm and through the silica gel with pore size of 15 nm. The obtained suspension was then placed in the dialysis sack with the pore size of 1 kDa and mixed in water for 8 h using magnetic stirrer for disposal of the residues of various chemical reaction products. Deionized water (Millipore Simplicity UV water purification system) was used for preparation of CD aqueous suspensions.

2.2. Experimental section

The X-ray Photoelectron Spectroscopy (XPS) measurements of dried CD were performed on a SPECS photoelectron spectrometer (Berlin, Germany) with using PHOIBOS-150-MCD-9 hemispherical analyzer and FOCUS-500 X-ray monochromator (AlK α radiation, $h\nu = 1486.74$ eV, 200 W).

The fluorescence spectra of the prepared CD suspensions were excited by diode laser radiation (wavelength 405 nm, laser power in the sample 50 mW) and recorded using CCS200 spectrometer (Thorlabs). The practical spectral resolution was 2 nm. The sample temperature in the cuvette varied from 22°C to 81°C using Peltier elements located on two opposite faces of the cuvette. Tempera-

ture control/measurement was performed using thermocouple placed directly in the suspension. The accuracy of the suspension temperature measurement was 0.3°C.

The value of the Zeta potential and size of nanoparticles in the suspension were determined using the Malvern ZetaSizer Nano ZS (Malvern, Worcestershire, UK).

Measurements of CD aqueous suspensions pH value were carried out using the ionometric converter Aquilon I-500 equipped with pH electrode (pH InLab Nano (Mettler Toledo)).

3. Results and discussion

3.1. CD aqueous suspensions characterization

To analyze the CD surface, XPS was used. Data obtained by XPS demonstrates that in the studied samples there are nitrogen (about 7% of total amount of atoms) and oxygen atoms (about 30%) in addition to carbon atoms. The XPS spectra analysis (spectral peaks of C1s (285 eV), N1s (399 eV), O1s (531 eV)) have revealed the presence of the following surface functional groups: C-H, C-N, C-OH, C = O, HO-C = O, O = C-OH, O-H, C-N-C (part of pyrolytic rings), N-H, N-C₃.

To study the effect of pH value changes on the CD FL, samples of CD suspensions with different pH values – from 5 to 9.21 – were prepared. For change the pH values, aqueous solutions of NaOH (Dia-M, concentration 10 mM, pH = 12) and 37% HCl (Sigma Aldrich, concentration 10 mM, pH = 2) were used. Measurements showed that the studied CD in the prepared aqueous suspension have negative Zeta potential (-30 mV) and hydrodynamic radius of 20 nm.

3.2. Dependence of fluorescence of CD aqueous suspensions on pH and temperature

This article studies the dependence of aqueous suspensions FL on the pH value ranging from 5 to 9.21 and on the temperature ranging from 22 to 81°C.

Fig. 1 shows the FL spectra of CD aqueous suspensions at different pH values of the suspensions. The FL spectra of CD aqueous suspensions under excitation by radiation with 405 nm wavelength represent broad structureless bands in the visible spectrum region with the maximum located near 520 nm. To process the FL spectra of CD aqueous suspensions one removed outliers, divided the signal intensity channel-by-channel by the area of the valence vibrations of water OH groups (460–476 nm) and smoothed the

spectra via the Savitsky-Goley method [23] (1st order polynomial, the window width was 51 channels – 11.4 nm). Presented data indicates a decrease of the FL intensity of CD aqueous suspensions at a constant temperature corresponding to an increase of the pH value of the suspension.

To analyze quantitatively the changes in the CD FL caused by the change of suspension pH value one used F0 parameter, equal to the ratio of the integral FL intensity to the integral intensity of the Raman band, originating from valent vibrations of OH-groups [24].

Fig. 2 shows the CD FL intensity decreasing linearly with the pH value increasing from 5 to 9.21 at the constant temperature. Such dependence of CD FL on pH value can be explained by the fact that pyridine nitrogen atoms in CD can gradually protonate under the pH value decrease. As a result, the possible proton transfer from protonated nitrogen to the conjugated carbon structure of CD increases the CD fluorescence [25].

It worth noting that the F0(pH) dependences differ for different temperatures (Fig. 2), indicating the intensity of CD FL in water is sensitive to changes of both pH and temperature of the samples. The complex dependence of CD FL on pH and temperature also follows from experiments on the influence of temperature on the FL intensity at constant pH values.

Fig. 3 indicates that, at the constant pH value, the intensity of CD FL decreases monotonously with increasing temperature. This may be caused by thermal activation of surface traps or defective CD states, as well as by thermally induced increase of the non-radiative excitation relaxation probability. At low temperatures, the non-radiative channel is deactivated, therefore, the transition of electrons from the excited state to the main state with emission of photons is possible. As soon as the temperature rises, non-radiative channels are activated, resulting in surface, defective, and ionized impurity states [26,27]. In this case, the probability of photon radiation during the transition of electrons to the ground state decreases.

The presented results on the influence of sample temperature on the CD FL intensity in water at different pH values demonstrated the complex nonlinear dependence of the CD FL on these two parameters. Thus, the dependences of CD FL in the aqueous suspension on pH and temperature indicate the high sensitivity of CD FL to changes of these parameters. And, therefore, CD can be used as fluorescent nanosensors of pH and ambient temperature. In order to develop such nanosensors, one has to solve the two-parameter inverse problem of fluorescence spectroscopy of CD aqueous suspensions. As it follows from Figs. 2 and 3, it is hard

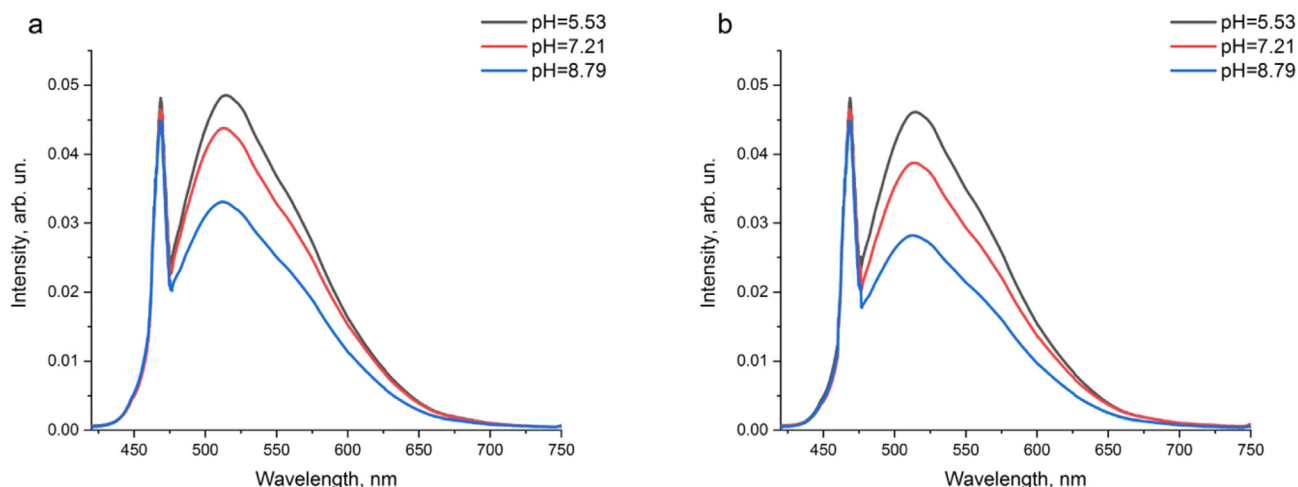


Fig. 1. FL spectra of CD aqueous suspensions a) suspension temperature 25 °C; b) suspension temperature 50 °C.

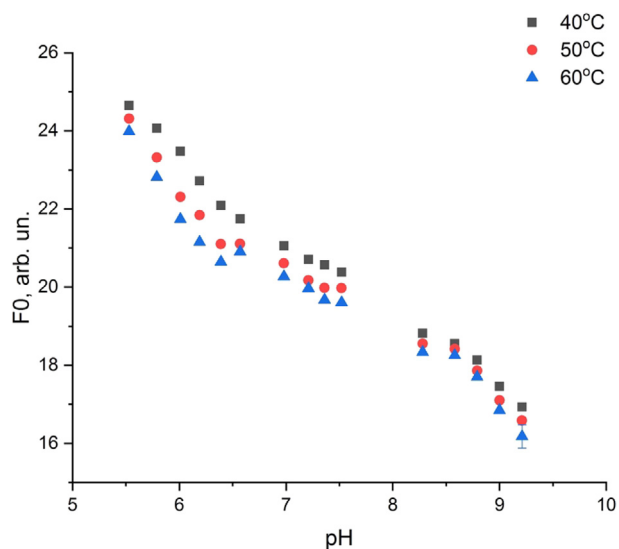


Fig. 2. CD aqueous suspension F0 parameter depending on the pH value at different temperatures: the temperature of the CD suspensions was 40 °C, 50 °C, 60 °C.

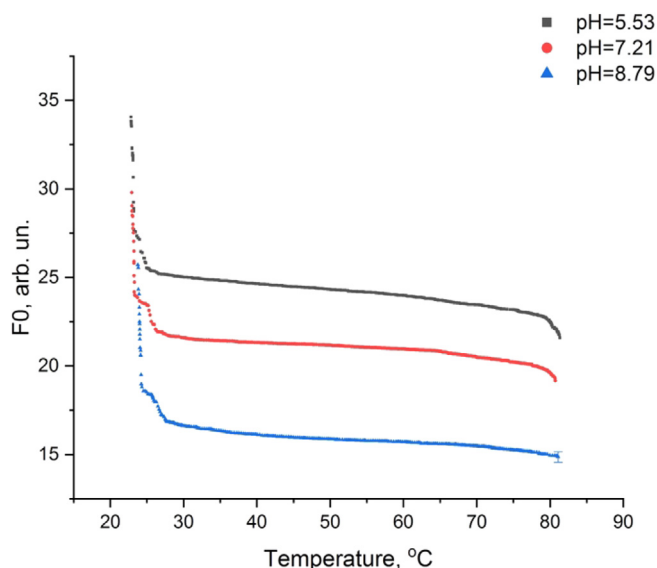


Fig. 3. Dependencies of the F0 parameter of the CD aqueous suspension on the temperature for different pH values.

to describe the complex dependencies $F_0(\text{pH}, T)$ by a specific analytical function and therefore to solve the specified inverse problem using conventional mathematical methods. That is why artificial neural networks were used to solve the problem.

3.3. ANNs application to solve the inverse problem of simultaneous determination of liquid medium pH and temperature values via CD fluorescence spectra

3.3.1. Preparing data for working with ANNs

As the result of fluorescence spectroscopy experiments, a total of 5600 FL spectra of CD aqueous suspensions with various pH and temperature values were obtained. The entire set of spectra consisted of 15 series, each corresponding to a fixed pH value from the following array: 5.53, 5.79, 6.01, 6.19, 6.39, 6.57, 6.98, 7.21, 7.36, 7.52, 8.28, 8.58, 8.79, 9.00, 9.21. Within each series with the same pH, the temperature of the suspensions varied between 22

and 81 °C with an uneven step that was hundredths of a degree. Each series with the same pH included between 234 and 462 examples.

The values of the FL intensity at the wavelengths ranging from 420 to 750 nm – a total of 1473 input features – were fed to the input of the ANN. Implementing supervised learning approach [28], one considered CD water suspension temperature and pH index to be the output features (Fig. 4). The entire dataset was randomly divided into training, validation, and test sets in the ratio of 70:20:10, respectively. One obtained experimental spectra of the training set – the spectrum of CD photoluminescence at pH = 6.98 and the temperature 24.7 – is presented in Supplemental Materials in Fig. S2 and full feature set for five experimental spectra used for ANNs training are present in Supplementary File.

3.3.2. ANN training

The authors used the model of a fully connected neural network (Sequential), implemented in the *keras* library [29]. This implies that each network neuron from the previous layer was connected to each neuron from the next layer. The configurations of networks with one hidden layer, two, and three hidden layers were considered. Multi-layer perceptrons (MLP) (for additional information the reader is referred to Supplementary materials) with one hidden layer (128, 64, 32, 16 neurons in it), two hidden layers (128 + 64, 64 + 32, 32 + 16 neurons in them) and three hidden layers (128 + 64 + 32, 64 + 32 + 16 neurons) were trained. Sigmoid was used as the activation function in the hidden layers, and a linear function was used in the output layer. We used ‘adam’ optimizer for the network training and mean absolute error as a loss function.

To prevent random data splitting into sets from affecting the results, the cross-validation method was implemented: the splitting was performed five times, and the results of ANN performance were averaged in these five cases.

To prevent overtraining of the ANN, the absence of error reduction on the validation set during 500 training epochs on the training set was used as a criterion for training termination.

In each case, 5 neural networks were trained in order to offset the impact of the weights initialization. Statistical indicators of the problem solution for all five networks were averaged in each case.

3.3.3. Approaches to solving the inverse problem and their comparative analysis

In general, different approaches can be used to solve N-parametric inverse problem of determining the values of N parameters: (1) simultaneous determination – all of the N output features are determined simultaneously via single ANN; (2) autonomous determination – N output feature are determined independently via N ANNs with one output each; (3) sequential determination – first of all, one determines the parameter that is best defined in the autonomous approach, the next parameter is determined by selecting examples from the database that correspond to the value of the first parameter determined at the previous step, and so on.; (4) group determination ($N \geq 3$) – an intermediate approach between simultaneous and autonomous ones, which involves combining output features into groups where features are defined simultaneously. The quality of the simultaneous determination of several output features is dependent on two factors: similarity of the defined dependencies for the features to be grouped, and coincidence of significant input features sets for the output features to be grouped [30].

The present paper compares the performance results of the ANNs trained according to (1) – (3) approaches. At the first stage, in all approaches (1) – (3), a perceptron with 16 neurons in a single hidden layer was trained. The mean absolute errors (MAE) (on the

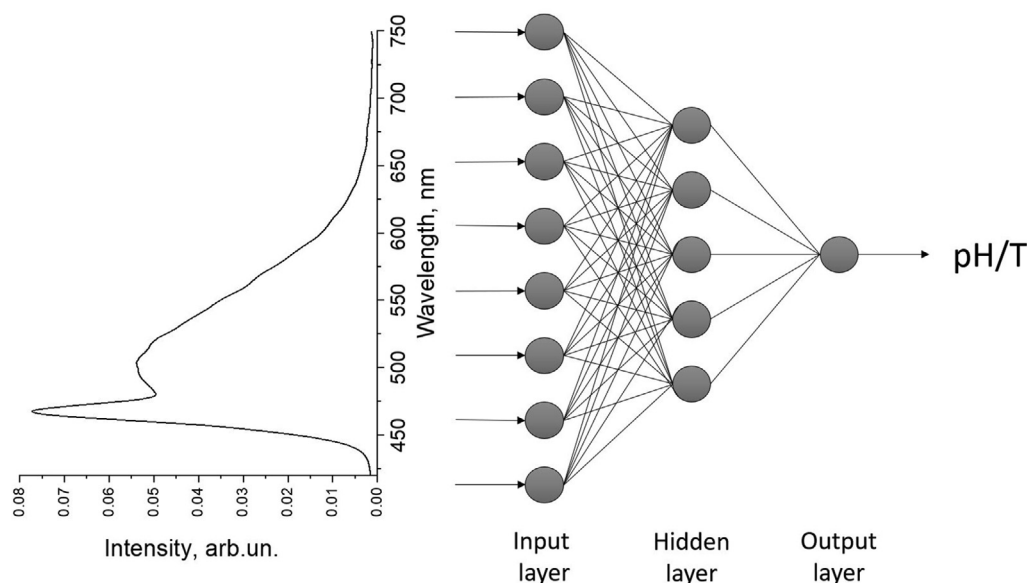


Fig. 4. Schematic representation of the ANN performance.

test set) of determining pH and temperature values corresponding to these approaches are shown in Fig. 5.

The results indicate that the sequential approach provides the smallest MAE of the output features determination (3) in comparison with simultaneous (1) and autonomous (2) ones. Thus, in the sequential approach, the pH error is 60% lower than the corresponding value in the simultaneous approach, and the temperature error is 70% lower. In terms of these results, the simultaneous approach was further used to solve the two-parameter inverse problem. At the first stage, the full dataset (5600 examples) was used to determine the hydrogen index of the medium. Then, examples corresponding to a certain pH value were selected from the full dataset, and a new dataset comprising the selected examples was formed. It was used to determine the suspension temperature (Fig. 6). Note that from the user's point of view, the simultaneous approach will not affect the device's operating time in any way.

Next, we conducted the selection of the optimal ANN architecture to solve the task. The training results are shown in Fig. 7.

By the analysis of the results presented in Fig. 8, the optimal perceptron architecture was selected for further research i.e.

architecture with a minimum MAE in determining pH and temperature. Thus, all further computations were performed with a perceptron with two hidden layers of 128 and 64 neurons in each. The use of this perceptron provided pH and temperature detection errors on the test set of 0.01 units and 1.36°C, respectively.

It should be noted that the obtained values represent already quite satisfactory results for simultaneous determination of pH and ambient temperature values from the CD FL spectra, as well as for biological tissue diagnostics. Recall that in living organisms, the pH varies from 4 to 8, and the temperature during inflammatory processes can vary up to 7°.

3.3.4. Reducing input data dimensionality

The quality of the inverse problem solution depends significantly on the input data dimensionality. Generally, not all input features are equally informative [31]. As the perceptron configuration selected at the previous step has a large number of synaptic weights, considering redundant uninformative features may lead to excessive complexity of the approximation function (i.e. ANN), which, eventually, may result in a decrease in the quality of the

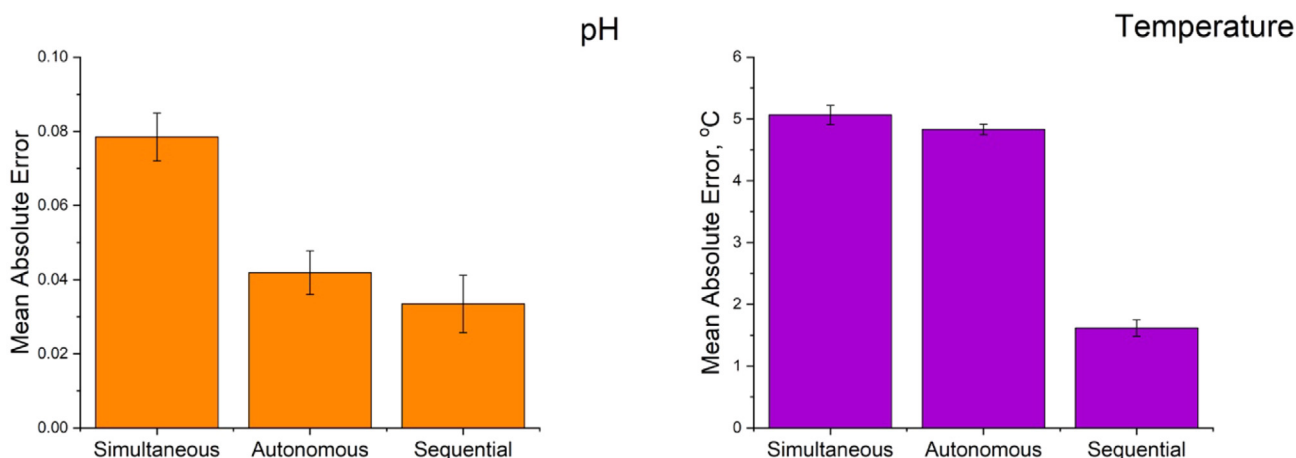


Fig. 5. Mean absolute error in pH and temperature determination for different approaches to solving the inverse problem. Test set, a perceptron with 16 neurons in a single hidden layer.

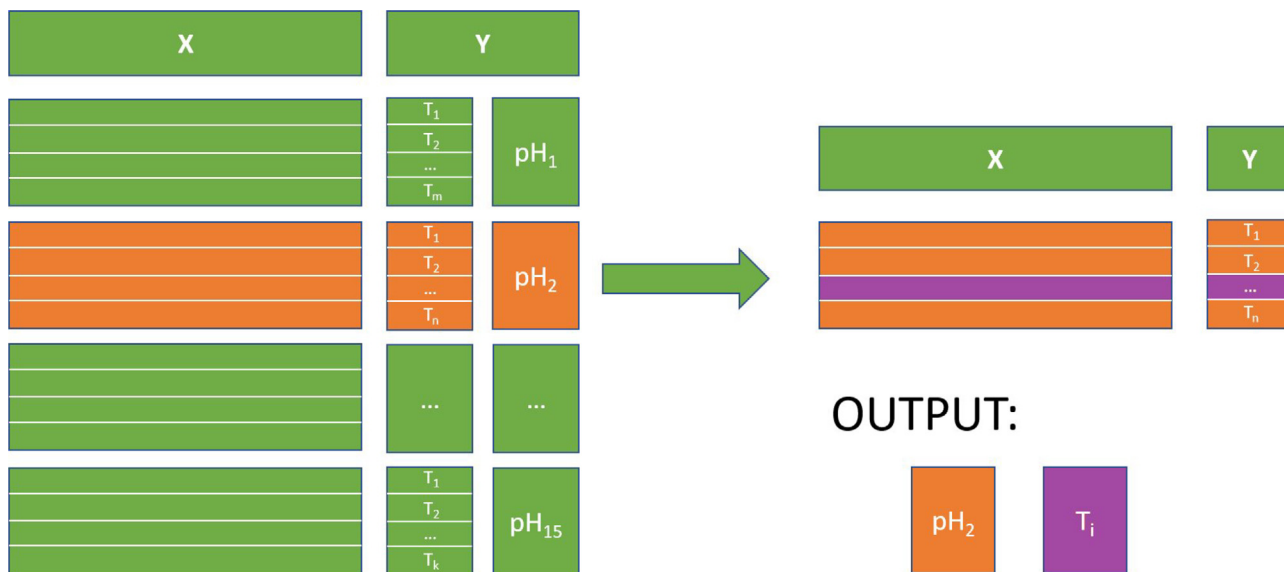


Fig. 6. Illustration of the simultaneous approach (3) implementation to determining the required parameters of the suspension used in the study.

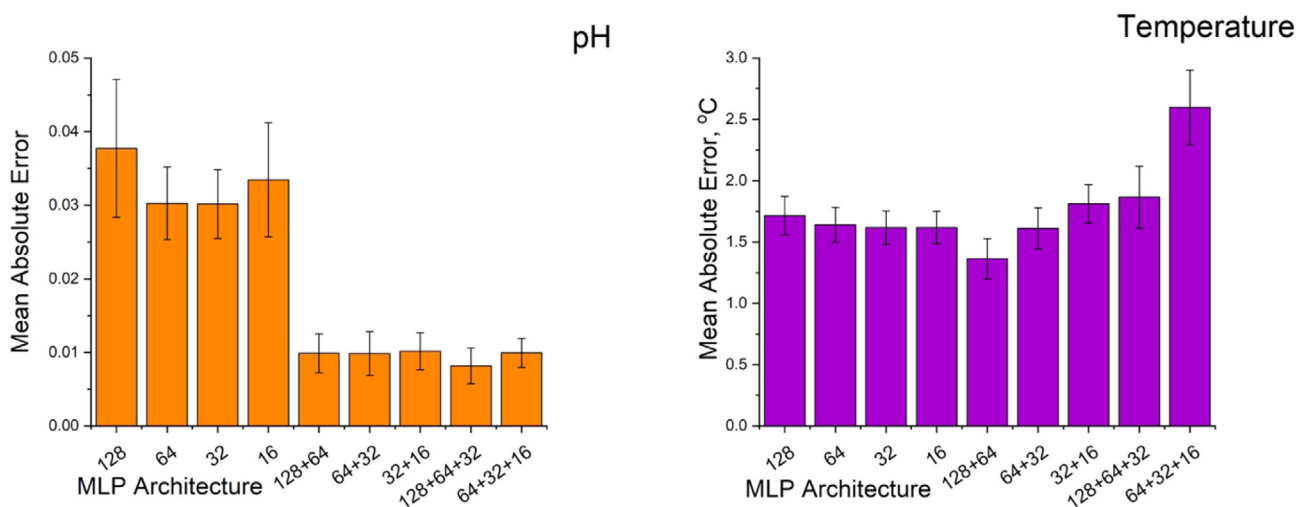


Fig. 7. MAE of pH and temperature determination, obtained on the test set after training MLPs of various architectures.

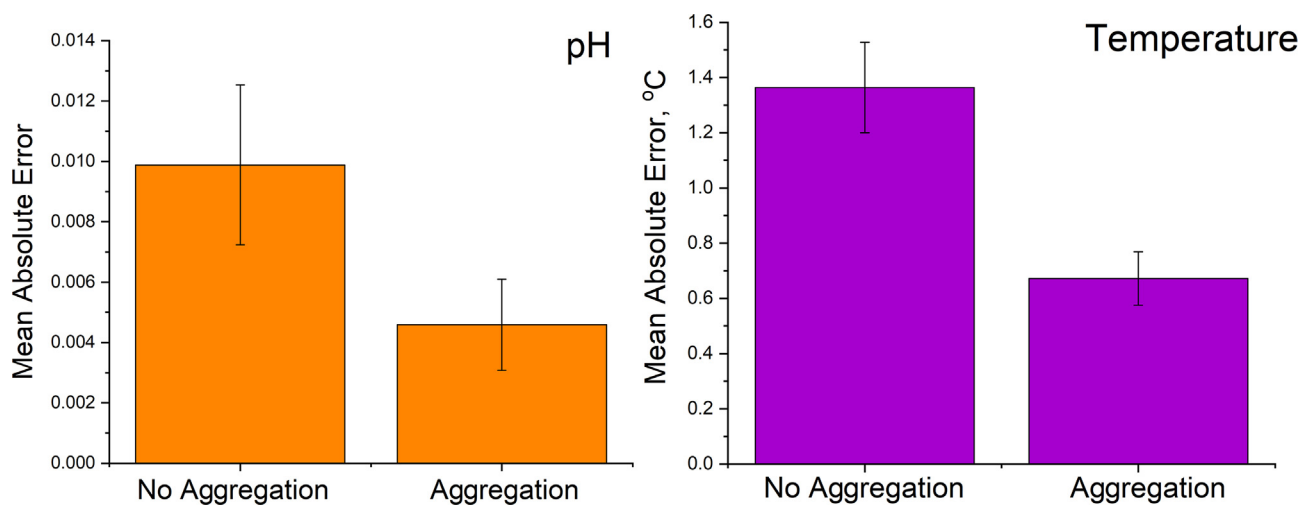


Fig. 8. MAE in determining pH and temperature obtained on the test set after reducing the input data dimensionality.

inverse problem solving. Indeed, note that the difference in wavelength between two neighboring channels is 0.22 nm (from the calculation that the spectral range of 330 nm accounts for 1473 spectral channels). However, a strong relationship between the values of the spectrum amplitude in closely spaced channels, arising from the actual spectrometer resolution is 2 nm (see 2.2.), means that their separate consideration does not lead to an increase in the amount of information received by the neural network. From the above, one can assume that reducing the number of input features by 10 times will simplify the approximation function, and, therefore, will reduce the error in determining pH and temperature of the suspensions.

To reduce the input dimensionality, an aggregation procedure was applied to the spectral data. It consisted of forming a new set of input features where every 10 input features values corresponding to 10 neighbouring spectral channels, were replaced with one, equal to the arithmetic average these 10 input features values. Thus, the input data dimensionality decreased from 1473 to 148. The results of ANN training on a corresponding dataset are shown in Fig. 8.

The presented results indicate that the aggregation procedure allowed to reduce MAE of temperature determination by 50.7%, pH – by 53.6% comparing to the use of a full input features set. Thus, the application of MLP (128 + 64 neurons in hidden layers) to the database of CD FL spectra, complemented with input dimensionality reduction procedure via aggregation of spectral channels, provided the determination of temperature and pH index of the medium from the single database with an error of 0.67°C and 0.005, respectively.

Comparing the obtained errors in determining pH and ambient temperature values with the literature data allows one to conclude that the results of the method proposed in this article are unique. According to the references, other groups have developed nanoprobes providing the determination of pH index as accurate as hundredths of a unit [4,5], while probes' temperature determination sensitivity varies from 0.4 to 0.7°C [8]. However, the nanoprobes determine these parameters separately: either only pH or only temperature. ANN application performed in the study provides simultaneous determination of these parameters (using the same experimental spectrum). Moreover, in our case, the sensor's operating temperature range is 1.5–2 times wider than in the above publications. This enables CD usage as pH and temperature sensors not only in biology and medicine, but also in various technological processes where it is necessary to control the conditions for the course of reactions, for example, in the process of molecular DNA calculations [32]. Obviously, narrowing the temperature range increases the accuracy of determining the medium temperature.

4. Conclusion

The paper demonstrates the successful application of fluorescence spectroscopy and ANNs to create a carbon-based nanosensor of environmental pH and temperature. We showed that the fluorescence of CD prepared via hydrothermal synthesis is sensitive to pH and water temperature changes. The ANN application for solving the two-parameter inverse problem of fluorescence spectroscopy provided simultaneous measurement of these parameters from CD FL spectra with high accuracy.

The optimal MLP architecture was found. It provided the smallest MAE values in determining temperature and pH, equal to $1.36 \pm 0.16^\circ\text{C}$ and 0.010 ± 0.003 units respectively, for the full features set.

Aggregation of input features over 10 channels allowed reducing MAE of temperature determination by 50.7%, pH – by 53.6%. Thus, the MLP application to the database of CD aqueous suspen-

sion FL spectra together with input dimensionality reduction provided simultaneous determination of environmental temperature and pH values with an accuracy of 0.67°C and 0.005, respectively. These results provide broad prospects for creating an optical multifunctional CD-based nanosensor.

CRedit authorship contribution statement

O.E. Sarmanova: Formal analysis, Software, Writing - original draft, Visualization, Data curation. **K.A. Laptinskiy:** Conceptualization, Methodology, Investigation, Visualization, Validation. **M.Y. Khmeleva:** Investigation, Formal analysis, Validation. **S.A. Burikov:** Investigation, Writing - review & editing, Funding acquisition, Validation. **S.A. Dolenko:** Supervision, Writing - review & editing, Funding acquisition. **A.E. Tomskaya:** Resources, Writing - review & editing. **T.A. Dolenko:** Conceptualization, Supervision, Resources, Writing - review & editing, Project administration, Funding acquisition.

Declaration of Competing Interest

The authors declare that they have no known competing financial interests or personal relationships that could have appeared to influence the work reported in this paper.

Acknowledgement

This study has been supported by Russian Foundation for Basic Research (Projects No. 20-32-70150 (K.A.Laptinskiy, T.A.Dolenko) and No. 19-01-00738 (S.A.Burikov, S.A.Dolenko)). The contribution of O.E.Sarmanova (programming and training of neural networks) was supported by the Foundation for the Advancement of Theoretical Physics and Mathematics "BASIS" (Project No. 19-2-6-6-1). This research was performed according to the Development program of the Interdisciplinary Scientific and Educational School of Lomonosov Moscow State University «Photonic and Quantum technologies. Digital medicine» (T.A.Dolenko).

Appendix A. Supplementary data

Supplementary data to this article can be found online at <https://doi.org/10.1016/j.saa.2021.119861>.

References

- [1] J.A. Kellum, Determinants of blood pH in health and disease, *Critical Care*. 4 (1) (2000) 6.
- [2] J. Allyn, D. Vandroux, J. Jabot, C. Brulliard, R. Galliot, X. Tabatchnik, et al., Prognosis of patients presenting extreme acidosis (pH <7) on admission to intensive care unit, *J. Crit. Care*. 31 (2016) 243–248.
- [3] N. Sperelakis, *Cell Physiology Source Book: Essentials of Membrane Biophysics*, fourth ed., Elsevier, 2011.
- [4] M.H. Lee, J.H. Han, J.H. Lee, N. Park, R. Kumar, C. Kang, J.S. Kim, Two-Color Probe to Monitor a Wide Range of pH Values in Cells, *Angew. Chem. Int. Edit.* 52 (24) (2013) 6206–6209.
- [5] J. Wen, P. Xia, Z. Zheng, Y. Xu, H. Li, F. Liu, S. Sun, Naphthalimide-rhodamine based fluorescent probe for ratiometric sensing of cellular pH, *Chinese Chem. Lett.* 28 (10) (2017) 2005–2008.
- [6] J.-W. Chen, C.-M. Chen, C.-C. Chang, A fluorescent pH probe for acidic organelles in living cells, *Org. Biomol. Chem.* 15 (2017) 7936–7943.
- [7] S.S. Evans, E.A. Repasky, D.T. Fisher, Fever and the thermal regulation of immunity: the immune system feels the heat, *Nat. Rev. Immunol.* 15 (6) (2015) 335–349.
- [8] S. Long, Y. Xu, F. Zhou, B. Wang, Y. Yang, Y. Fu, et al., Characteristics of temperature changes in photothermal therapy induced by combined application of indocyanine green and laser, *Oncol. Lett.* 17 (2019) 3952–3959.
- [9] O.E. Sarmanova, S.A. Burikov, K.A. Laptinskiy, O.D. Kotova, E.A. Filippova, T.A. Dolenko, In vitro temperature sensing with up-conversion $\text{NaYF}_4:\text{Yb}^{3+}/\text{Tm}^{3+}$ -based nanocomposites: Peculiarities and pitfalls, *Spectrochim. Acta A* 241 (2020) 118627.

- [10] J.S. Donner, S.A. Thompson, M.P. Kreuzer, G. Baffou, R. Quidant, Mapping Intracellular Temperature Using Green Fluorescent Protein, *Nano Lett.* 12 (4) (2012) 2107–2111.
- [11] S. Wang, I.S. Cole, Q. Li, The toxicity of graphene quantum dots, *RSC Adv.* 6 (92) (2016) 89867–89878.
- [12] S.K. Tammina, D. Yang, X. Li, S. Koppala, Y. Yang, High photoluminescent nitrogen and zinc doped carbon dots for sensing Fe³⁺ ions and temperature, *Spectrochim. Acta A* 222 (2019) 117141.
- [13] J.-R. Macairan, D.B. Jaunky, A. Piekny, R. Naccache, Intracellular ratiometric temperature sensing using fluorescent carbon dots, *Nanoscale Adv.* 1 (1) (2019) 105–113.
- [14] W.-J. Wang, J.-M. Xia, J.i. Feng, M.-Q. He, M.-L. Chen, J.-H. Wang, Green preparation of carbon dots for intracellular pH sensing and multicolor live cell imaging, *J. Mater. Chem. B* 4 (44) (2016) 7130–7137.
- [15] T. Dolenko, S. Burikov, K. Laptinskiy, J.M. Rosenholm, O. Shenderova, I. Vlasov, Evidence of carbon nanoparticle – solvent molecule interactions in Raman and fluorescence spectra, *Phys. Status Solidi A* 212 (11) (2015) 2512–2518.
- [16] M. Gniadecka, P.A. Philipsen, S. Sigurdsson, S. Wessel, O.F. Nielsen, D.H. Christensen, et al., Melanoma diagnosis by Raman spectroscopy and neural networks: structure alterations in proteins and lipids in intact cancer tissue, *J. Invest. Derm.* 122 (2004) 443.
- [17] M.B. Takahashi, J. Leme, C.P. Caricati, A. Tonso, E.G. Fernández Núñez, J.C. Rocha, Artificial neural network associated to UV/Vis spectroscopy for monitoring bioreactions in biopharmaceutical processes, *Bioproc. Biosyst. Eng.* 38 (6) (2015) 1045–1054.
- [18] K. Laptinskiy, S. Burikov, S. Dolenko, A. Efitorov, O. Sarmanova, O. Shenderova, I. Vlasov, T. Dolenko, Monitoring of nanodiamonds in human urine using artificial neural networks, *Phys. Status Solidi A* 213 (10) (2016) 2614–2622.
- [19] O.E. Sarmanova, S.A. Burikov, S.A. Dolenko, I.V. Isaev, K.A. Laptinskiy, N. Prabhakar, D.Ş. Karaman, J.M. Rosenholm, O.A. Shenderova, T.A. Dolenko, A method for optical imaging and monitoring of the excretion of fluorescent nanocomposites from the body using artificial neural networks, *Nanomed.-Nanotechnol.* 14 (4) (2018) 1371–1380.
- [20] T. Munro, L. Liu, C. Glorieux, H. Ban, CdSe/ZnS quantum dot fluorescence spectra shape-based thermometry via neural network reconstruction, *J. Appl. Phys.* 119 (2016) 214903.
- [21] A. Barati, M. Shamsipur, H. Abdollahi, Carbon dots with strong excitation-dependent fluorescence changes towards pH. Application as nanosensors for a broad range of pH, *Anal. Chim. Acta* 931 (2016) 25–33.
- [22] A.E. Tomskeya, I.P. Prosvirin, M.N. Egorova, S.A. Smagulova, I.P. Asanov, Structural and Optical Properties of N-Doped and B-Doped Carbon Dots, *J. Struct. Chem.* 61 (5) (2020) 818–825.
- [23] A. Savitzky, M.J.E. Golay, Smoothing and differentiation of data by simplified least squares procedures, *Anal. Chem.* 36 (8) (1964) 1627–1639.
- [24] T. Dolenko, S. Burikov, K. Laptinskiy, J.M. Rosenholm, O. Shenderova, I. Vlasov, Evidence of carbon nanoparticle–solvent molecule interactions in Raman and fluorescence spectra, *Phys. Status Solidi A* 212 (11) (2015) 2512–2518.
- [25] Z. Qian, J. Ma, X. Shan, H. Feng, L. Shao, J. Chen, Highly luminescent N-doped carbon quantum dots as an effective multifunctional fluorescence sensing platform, *Chem.–Eur. J.* 20 (8) (2014) 2254–2263.
- [26] K. Chan, S. Yap, K. Yong, Biogreen Synthesis of Carbon Dots for Biotechnology and Nanomedicine Applications, *Nano-Micro Lett.* 10 (2018) 72.
- [27] R.M.S. Sendão, D.M.A. Crista, A.C.P. Afonso, M.D.V. Martínez de Yuso, M. Algarra, J.C.G. Esteves da Silva, L. Pinto da Silva, Insight into the hybrid luminescence showed by carbon dots and molecular fluorophores in solution, *Phys. Chem. Chem. Phys.* 21 (37) (2019) 20919–20926.
- [28] S. Haykin, *Neural Networks: A Comprehensive Foundation*, second ed., Prentice Hall International Inc, 2004.
- [29] Keras 2.0.8. Documentation, Sequential – keras 2.0.8. Documentation. <https://faroit.com/keras-docs/2.0.8/models/sequential/>, 2021 (accessed 11 April 2021).
- [30] A. Efitorov, S. Burikov, T. Dolenko, K. Laptinskiy, S. Dolenko, Significant feature selection in neural network solution of an inverse problem in spectroscopy, *Procedia Comput. Sci.* 66 (2015) 93–102.
- [31] S. Dolenko, I. Isaev, E. Osborne, I. Persiantsev, M. Shimelevich, Study of influence of parameter grouping on the error of neural network solution of the inverse problem of electrical prospecting, *Commun. Comput. Inf. Sci.* 383 (2013) 81–90.
- [32] T. Dolenko, S. Burikov, E. Vervalde, A. Efitorov, K. Laptinskiy, O. Sarmanova, et al., Improvement of reliability of molecular DNA computing: solution of inverse problem of Raman spectroscopy using artificial neural networks, *Laser Phys.* 27 (2017) 025203.